Available online at www.sciencedirect.com
ScienceDirect
Journal of Sound and Vibration 324 (2009) 733–750
JOURNAL OF SOUND AND VIBRATION
www.elsevier.com/locate/jsvi

Three-dimensional vibration analysis of functionally graded material plates in thermal environment

Q. Li, V.P. Iu*, K.P. Kou

Department of Civil and Environmental Engineering, University of Macau, Av. Padre Tomás Pereira S.J., Taipa, Macao SAR, PRC

Received 5 December 2007; received in revised form 26 November 2008; accepted 22 February 2009
Handing Editor: L.G. Tham
Available online 1 April 2009

Abstract

Free vibration of functionally graded material rectangular plates with simply supported and clamped edges in the thermal environment is studied based on the three-dimensional linear theory of elasticity. Simply supported and clamped FGM plates with temperature-dependent material properties subjected to uniform temperature rise, linear temperature rise and nonlinear temperature rise are considered. The three displacements of the plates are expanded by a series of Chebyshev polynomials multiplied by appropriate functions to satisfy the essential boundary conditions. The natural frequencies are obtained by Ritz method. The numerical results of the present approach are compared with the results of other researchers for the validation. Parametric study is performed for supported conditions, temperature fields, volume fraction indices of FGM plates.

1. Introduction

Functionally graded materials (FGMs) were first introduced by a group of Japanese scientists in 1984 [1,2], as ultrahigh temperature resistant materials for aircraft, space vehicles and other engineering applications. These kinds of materials are heterogeneous composite materials, in which the material properties vary continuously and smoothly from one interface to the other. This is achieved by gradually varying the volume fraction of the constituent materials. Because of this advantage, they have been regarded as one of the advanced inhomogeneous composite materials in many engineering sectors.

FGMs were originally designed as thermal barrier materials for aerospace structural applications and fusion reactors. Nowadays, they are developed for the general use as structural components in high-temperature environment. Many studies for thermal stress, thermal bending, and vibration of FGM plates are available in the literature. Numerous studies on free vibration for isotropic and composite multilayered plates with or without initial thermal and/or mechanical in-plane loads have been reported. Among these, Praveen and Reddy [3] conducted the nonlinear transient thermoelastic analysis of functionally graded ceramic–metal plates using a plate finite element. Reddy [4] presented a general formulation for FGM plates using the

*Corresponding author. Tel.: +853 397 4301; fax: +853 831 694.
E-mail address: vaipaniu@umac.mo (V.P. Iu).

0022-460X/$ - see front matter © 2009 Elsevier Ltd. All rights reserved.
doi:10.1016/j.jsv.2009.02.036

third-order shear deformation plate theory and developed the associated finite element model that accounts for the thermomechanical coupling and geometric nonlinearity. However, they did not consider the change of material properties due to temperature distribution in the analysis. Yang and Shen [5] analyzed the vibration characteristics and transient response of shear deformable FGM plates made of temperature-dependent materials in thermal environment. Huang and Shen [6] dealt with the nonlinear vibration and dynamic response of FGM plates in thermal environment based on the higher-order shear deformation plate theory and general von Kármán-type equation. Kim [7] investigated vibration characteristics of initially stressed FGM rectangular plates in thermal environment by using Rayleigh–Ritz method based on the third-order shear deformation plate theory to account for rotary inertia and transverse shear strains.

There are also several studies about finding the three-dimensional exact solutions for FGM plates. Reddy and Cheng [8] obtained a three-dimensional solution of a smart FGM plate consisting of a plate made of FGM and actuators made of an active material by the combination of the transfer matrix formulation and asymptotic expansion. Vel and Batra [9] presented a three-dimensional exact solution for free and forced vibrations of simply supported FGM rectangular plates by using suitable displacement functions to reduce equations governing steady-state vibration of the plate.

However, the three-dimensional analysis of the free vibration of FGM plates in the thermal environments is limited in number in the open literature. In the present study, the three-dimensional vibration analysis of rectangular FGM plates in the thermal environments is carried out based on Ritz method. The power-law FGM plates with two support conditions—simply supported and clamped—and the temperature-dependent material properties are considered. The three displacements of rectangular plates are expanded by Chebyshev polynomial series multiplied by boundary functions [10,11]. The present approach is validated by the comparisons of the published literature. The effects of volume fraction indices, supported conditions, thickness-side ratios, aspect ratios and temperature changes are also discussed in the parametric study.

2. Problem statement

2.1. Geometrical configuration

Consider a rectangular FGM plate with the uniform thickness, which is referred in a rectangular coordinates (x_1, x_2, x_3) and vibrating in the thermal environment. The length, width and thickness of the plate are a, b, and h, respectively. The bottom and top surfaces of the plate are bounded by the planes $x_3 = \pm h/2$, and axes are parallel to the edges of the plate. The displacement components at generic points are u_1, u_2, and u_3 corresponding to the x_1, x_2, and x_3 directions.

For simplicity and generality, the non-dimensional parameters are introduced

$$\xi = \frac{2x_1}{a}, \quad \eta = \frac{2x_2}{b}, \quad \zeta = \frac{2x_3}{h} \tag{1}$$

where $\xi, \eta, \zeta \in [-1, 1]$.

2.2. Temperature field across the thickness

There are three cases considering the temperature change across the thickness of plate.

2.2.1. Uniform temperature rise

The initial uniform temperature of the plate is assumed to be T_0 ($T_0 = 300\,\mathrm{K}$). The temperature field is expressed as

$$T = T_0 + \Delta T \tag{2}$$

where ΔT denotes the temperature change.

2.2.2. Linear temperature rise

Assuming the temperature T_b and T_t at the bottom and top of the plate, the temperature field under linear temperature rise in x_3-direction is expressed as

$$T(\zeta) = T_b + \Delta T \cdot \left(\frac{\zeta}{2} + \frac{1}{2}\right) \tag{3}$$

where $\Delta T = T_t - T_b$ is the temperature gradient; T_b equals the initial temperature 300 K.

2.2.3. Nonlinear temperature rise

The nonlinear temperature rise across the thickness of the plate is determined by solving the one-dimensional heat conduction equation. The equation for the temperature through the thickness is

$$-\frac{\mathrm{d}}{\mathrm{d}x_3}\left(\hat{k}(x_3)\frac{\mathrm{d}T}{\mathrm{d}x_3}\right) = 0 \tag{4}$$

where $T = T_t$ at the top face ($x_3 = h/2$) and $T = T_b$ at the bottom face ($x_3 = -h/2$), T_b is assumed to be the initial temperature 300 K. The thermal conductivity $\hat{k}(x_3)$ is given by Eq. (10). The analytical solution to Eq. (4) is

$$T(x_3) = T_t - (T_t - T_b)\frac{\int_{-h/2}^{x_3} \frac{1}{\hat{k}(x_3)}\mathrm{d}x_3}{\int_{-h/2}^{h/2} \frac{1}{\hat{k}(x_3)}\mathrm{d}x_3} \tag{5}$$

This equation does not take the temperature dependence of the material properties into account. As indicated in the work by Miyamoto et al. [12], this will not have a significant effect on results. The one-dimensional steady-state heat conduction equation (4) is first solved before the thermal analysis is carried.

In the case of power-law FGMs, the solution to Eq. (4) also can be expressed by means of polynomial series [13]

$$\begin{aligned} T(\zeta) = T_b + \frac{T_t - T_b}{C_{tb}}\Bigg[&\left(\frac{\zeta}{2}+\frac{1}{2}\right) - \frac{\hat{k}_{tb}}{(\kappa+1)\hat{k}_b}\left(\frac{\zeta}{2}+\frac{1}{2}\right)^{\kappa+1} \\ &+ \frac{\hat{k}_{tb}^2}{(2\kappa+1)\hat{k}_b^2}\left(\frac{\zeta}{2}+\frac{1}{2}\right)^{2\kappa+1} - \frac{\hat{k}_{tb}^3}{(3\kappa+1)\hat{k}_b^3}\left(\frac{\zeta}{2}+\frac{1}{2}\right)^{3\kappa+1} \\ &+ \frac{\hat{k}_{tb}^4}{(4\kappa+1)\hat{k}_b^4}\left(\frac{\zeta}{2}+\frac{1}{2}\right)^{4\kappa+1} - \frac{\hat{k}_{tb}^5}{(5\kappa+1)\hat{k}_b^5}\left(\frac{\zeta}{2}+\frac{1}{2}\right)^{5\kappa+1}\Bigg] \end{aligned} \tag{6}$$

with

$$C_{tb} = 1 - \frac{\hat{k}_{tb}}{(\kappa+1)\hat{k}_b} + \frac{\hat{k}_{tb}^2}{(2\kappa+1)\hat{k}_b^2} - \frac{\hat{k}_{tb}^3}{(3\kappa+1)\hat{k}_b^3} + \frac{\hat{k}_{tb}^4}{(4\kappa+1)\hat{k}_b^4} - \frac{\hat{k}_{tb}^5}{(5\kappa+1)\hat{k}_b^5} \tag{7}$$

where $\hat{k}_{tb} = \hat{k}_t - \hat{k}_b$, $\hat{k}_t$ and $\hat{k}_b$ are the thermal conductivity of the top and bottom faces of the plate, respectively; κ is the volume fraction index of power-law FGMs, which is described in Eq. (8).

The variations of temperature fields under three temperature rises along the thickness direction are plotted in Fig. 1. The nonlinear temperature rise is dependent of volume fraction index κ. However, the effect of κ is not significant as shown in Fig. 1 which plots the curves of different κ (0.2, 2, 10). It is also shown that the curve of linear temperature rise is very close to those of nonlinear temperature rises.

2.3. Material properties

The properties of general FGM plates vary continuously due to gradually changing the volume fraction of the constituent materials, usually in the thickness direction only. Power-law function [14,15] is commonly used

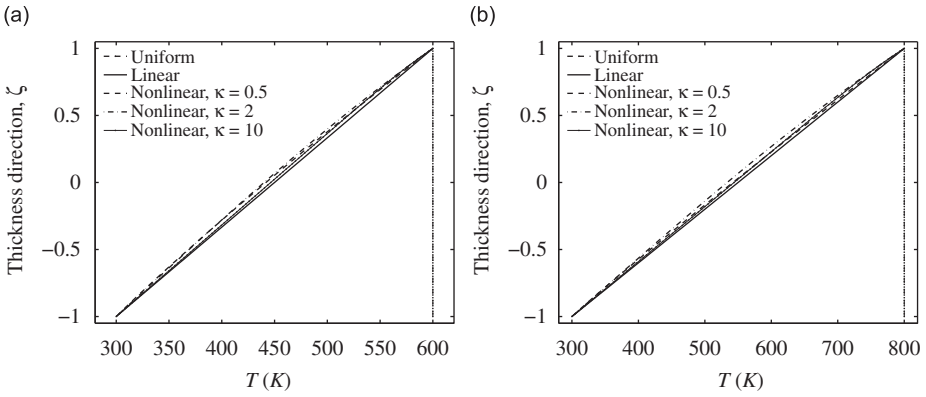

Fig. 1. The variations of temperature along the thickness direction with the initial temperature $T_0 = 300\,\mathrm{K}$: (a) temperature change $\Delta T = 300\,\mathrm{K}$; (b) temperature change $\Delta T = 500\,\mathrm{K}$.

to describe these variations of material properties as

$$g(\zeta) = \left(\frac{\zeta}{2} + \frac{1}{2}\right)^{\kappa} \tag{8}$$

where κ is the volume fraction index ($0 \leqslant \kappa \leqslant +\infty$), which dictates the material variation profile through the plate thickness.

The material properties—Young's modulus E, Poisson's ratio v, and thermal expansion coefficient α—are nonlinear functions of temperature $\mathscr{P}(T)$ [16] as

$$\mathscr{P}(T) = \mathscr{P}_0^T\left(\mathscr{P}_{-1}^T\frac{1}{T} + 1 + \mathscr{P}_1^T T + \mathscr{P}_2^T T^2 + \mathscr{P}_3^T T^3\right) \tag{9}$$

where $T = T_0 + \Delta T$ indicates the environmental temperature, and T_0 is the temperature of free stress state ($T_0 = 300\,\mathrm{K}$); $\mathscr{P}_0^T$, $\mathscr{P}_{-1}^T$, $\mathscr{P}_1^T$, $\mathscr{P}_2^T$, and $\mathscr{P}_3^T$ are the constants in the cubic expression of the specific temperature-dependent material property. Based on the rule of mixture [17], the effective material properties are expressed as

$$\mathscr{P}_{\mathrm{eff}}(\zeta, T) = \mathscr{P}_b(T) + [\mathscr{P}_t(T) - \mathscr{P}_b(T)]g(\zeta) \tag{10}$$

where $\mathscr{P}_{\mathrm{eff}}$ is the effective material properties of FGM at the temperature T, $\mathscr{P}_t$ and $\mathscr{P}_b$ are the properties of the top and bottom faces at the temperature T, respectively.

In the present study, it is assumed that the effective Young's modulus E, Poisson's ratio v, and thermal expansion coefficient α are temperature-dependent, whereas the mass density ρ and thermal conductivity $\hat{k}$ are independent of the temperature:

$$E(\zeta, T) = E_b(T) + [E_t(T) - E_b(T)]g(\zeta) \tag{11a}$$

$$v(\zeta, T) = v_b(T) + [v_t(T) - v_b(T)]g(\zeta) \tag{11b}$$

$$\alpha(\zeta, T) = \alpha_b(T) + [\alpha_t(T) - \alpha_b(T)]g(\zeta) \tag{11c}$$

$$\rho(\zeta) = \rho_b + [\rho_t - \rho_b]g(\zeta) \tag{11d}$$

$$\hat{k}(\zeta) = \hat{k}_b + [\hat{k}_t - \hat{k}_b]g(\zeta) \tag{11e}$$

Silicon nitride (Si_3N_4) and stainless steel (SUS304) are chosen to be the constituent materials of the FGM plates. The typical values of temperature-dependent coefficients are tabulated in Table 1 [5]. The effective material properties of linear and nonlinear temperature rises are still very close as well as the temperature distributions of linear and nonlinear rises. For example, the difference between the effective Young's modulus of linear and nonlinear temperature rises is about 1%.

Table 1
Temperature-dependent coefficients of Young's modulus E (Pa), Poisson's ratio ν, thermal expansion coefficient α (1/K), mass density ρ (kg/m^3) and thermal conductivity $\hat{k}$ (W/(m K)) of Si_3N_4 and SUS304 [5].

Material	$\mathscr{P}_{-1}^T$	$\mathscr{P}_0^T$	$\mathscr{P}_1^T$	$\mathscr{P}_2^T$	$\mathscr{P}_3^T$	$\mathscr{P}$ (at 300 K)
Si_3N_4						
E	0	348.43×10^9	-3.070×10^{-4}	2.160×10^{-7}	-8.946×10^{-11}	322.2715×10^9
ν	0	0.2400	0	0	0	0.2400
α	0	5.8723×10^{-6}	9.095×10^{-4}	0	0	7.4746×10^{-6}
ρ	0	2370	0	0	0	2370
$\hat{k}$	0	9.19	0	0	0	9.19
SUS304						
E	0	201.04×10^9	3.079×10^{-4}	-6.534×10^{-7}	0	207.7877×10^9
ν	0	0.3262	-2.002×10^{-4}	3.797×10^{-7}	0	0.3178
α	0	12.330×10^{-6}	8.086×10^{-4}	0	0	1.5321×10^{-5}
ρ	0	8166	0	0	0	8166
$\hat{k}$	0	12.04	0	0	0	12.04

3. Solution methodology

Considering the heating process in the current case, it can be separated into two stages: (1) the plate is heated firstly and (2) then vibrates in the static heated status. From this point of view, the displacement components are composed of the initial deformation U_i^0 due to the temperature change and periodic displacement components $\widetilde{U}_i\,\mathrm{e}^{\mathrm{i}\omega t}$:

$$\begin{aligned} u_1(\xi,\eta,\zeta,t) &= U_1^0(\xi,\eta,\zeta) + \widetilde{U}_1(\xi,\eta,\zeta)\,\mathrm{e}^{\mathrm{i}\omega t} \\ u_2(\xi,\eta,\zeta,t) &= U_2^0(\xi,\eta,\zeta) + \widetilde{U}_2(\xi,\eta,\zeta)\,\mathrm{e}^{\mathrm{i}\omega t} \\ u_3(\xi,\eta,\zeta,t) &= U_3^0(\xi,\eta,\zeta) + \widetilde{U}_3(\xi,\eta,\zeta)\,\mathrm{e}^{\mathrm{i}\omega t} \end{aligned} \tag{12}$$

where the displacement amplitude functions U_i^0 and $\widetilde{U}_i$ are expanded as triplicate summations of Chebyshev polynomial series multiplied by the boundary functions:

$$\begin{aligned} U_1^0(\xi,\eta,\zeta) &= \mathscr{R}_{u_1}\sum_{i=1}^{\infty}\sum_{j=1}^{\infty}\sum_{k=1}^{\infty} A_{ijk}^0 P_i(\xi)P_j(\eta)P_k(\zeta) \\ U_2^0(\xi,\eta,\zeta) &= \mathscr{R}_{u_2}\sum_{l=1}^{\infty}\sum_{m=1}^{\infty}\sum_{n=1}^{\infty} B_{lmn}^0 P_l(\xi)P_m(\eta)P_n(\zeta) \\ U_3^0(\xi,\eta,\zeta) &= \mathscr{R}_{u_3}\sum_{p=1}^{\infty}\sum_{q=1}^{\infty}\sum_{r=1}^{\infty} C_{pqr}^0 P_p(\xi)P_q(\eta)P_r(\zeta) \end{aligned} \tag{13}$$

$$\begin{aligned} \widetilde{U}_1(\xi,\eta,\zeta) &= \mathscr{R}_{u_1}\sum_{i=1}^{\infty}\sum_{j=1}^{\infty}\sum_{k=1}^{\infty} \widetilde{A}_{ijk} P_i(\xi)P_j(\eta)P_k(\zeta) \\ \widetilde{U}_2(\xi,\eta,\zeta) &= \mathscr{R}_{u_2}\sum_{l=1}^{\infty}\sum_{m=1}^{\infty}\sum_{n=1}^{\infty} \widetilde{B}_{lmn} P_l(\xi)P_m(\eta)P_n(\zeta) \\ \widetilde{U}_3(\xi,\eta,\zeta) &= \mathscr{R}_{u_3}\sum_{p=1}^{\infty}\sum_{q=1}^{\infty}\sum_{r=1}^{\infty} \widetilde{C}_{pqr} P_p(\xi)P_q(\eta)P_r(\zeta) \end{aligned} \tag{14}$$

in which $\mathscr{R}_\delta$ ($\delta = u_1, u_2, u_3$) are boundary functions to satisfy the essential boundary conditions along the edges; A^0_{ijk}, B^0_{lmn}, and C^0_{pqr} are the initial displacement coefficients which can be found while the temperature field and boundary supported conditions are determined; $\widetilde{A}_{ijk}$, $\widetilde{B}_{lmn}$, and $\widetilde{C}_{pqr}$ are the unknown coefficients to be determined; P_i ($i = 1, 2, 3, \ldots$) is the one-dimensional ith Chebyshev polynomial [18]:

$$P_i(x) = \cos[(i-1)\arccos(x)] \tag{15}$$

Chebyshev polynomials $P_i(x)$ are a set of complete and orthogonal function in the interval $[-1, 1]$. These polynomials showed some advantages such as high convergence rate and stability in the analysis of isotropic plates [10,11]. In the authors' analysis of FGM plates and FGM sandwich plates [19,20], these polynomials also showed the high convergence rate and stability.

For Ritz method, the essential boundary conditions for simply supported (referred to SSSS) and clamped (referred to CCCC) plates considered in the present study are

$$\begin{aligned} &u_2 = u_3 = 0 \quad \text{at } x_1 = \pm a/2 \\ &u_1 = u_3 = 0 \quad \text{at } x_2 = \pm b/2 \end{aligned} \quad \text{for simply supported condition} \tag{16a}$$

$$\begin{aligned} &u_1 = u_2 = u_3 = 0 \quad \text{at } x_1 = \pm a/2 \\ &u_1 = u_2 = u_3 = 0 \quad \text{at } x_2 = \pm b/2 \end{aligned} \quad \text{for clamped condition} \tag{16b}$$

The corresponding R-functions of these two boundary conditions are tabulated in Table 2.

The linear strain–displacement relation is

$$\varepsilon_{ij} = \tfrac{1}{2}(u_{i,j} + u_{j,i}) \tag{17}$$

Considering the heating process, the plate is heated firstly and then vibrates in the static heated status. The initial strain energy is

$$\mathscr{U}^0 = \frac{1}{2}\int_V [\sigma^0_{11}(\varepsilon^0_{11} - \alpha\Delta T) + \sigma^0_{22}(\varepsilon^0_{22} - \alpha\Delta T) + 2\sigma^0_{23}\varepsilon^0_{23} + 2\sigma^0_{31}\varepsilon^0_{31} + 2\sigma^0_{12}\varepsilon^0_{12}]\,\mathrm{d}V \tag{18}$$

when the plate is heated into the steady state firstly. If the temperature change ΔT has been applied, the plate will bend with the initial deflection and the corresponding initial thermal stresses arise because of the constraints of the boundary supports. Applying the principle of the minimize potential energy in the absence of kinetic energy

$$\frac{\partial \mathscr{U}^0}{\partial A^0_{ijk}} = 0, \quad \frac{\partial \mathscr{U}^0}{\partial B^0_{lmn}} = 0, \quad \frac{\partial \mathscr{U}^0}{\partial C^0_{pqr}} = 0 \quad (i,j,k,l,m,n,p,q,r = 1, 2, 3, \ldots) \tag{19}$$

leads to a set of linear equations:

$$\begin{aligned} \mathbf{K}^0_{11}\mathbf{A}^0 + \mathbf{K}^0_{12}\mathbf{B}^0 + \mathbf{K}^0_{13}\mathbf{C}^0 &= \mathbf{T}^0_1 \\ \mathbf{K}^0_{21}\mathbf{A}^0 + \mathbf{K}^0_{22}\mathbf{B}^0 + \mathbf{K}^0_{23}\mathbf{C}^0 &= \mathbf{T}^0_2 \\ \mathbf{K}^0_{31}\mathbf{A}^0 + \mathbf{K}^0_{32}\mathbf{B}^0 + \mathbf{K}^0_{33}\mathbf{C}^0 &= \mathbf{0} \end{aligned} \tag{20}$$

$\mathbf{K}^0_{ij}$, which are dependent of temperature, are the elements of the initial stiffness matrix when the plate is subjected to the steadily risen temperature field. $\mathbf{T}^0_1$ and $\mathbf{T}^0_2$ are the terms due to the temperature rise with the boundary support constraints. Solving for $\mathbf{C}^0$ and substitute into the first and second equations, Eq. (20) is

Table 2
Boundary R-functions for different boundary conditions.

BC	R-functions
Simply supported (SSSS)	$\mathscr{R}_{u_1} = 1-\eta^2$, $\mathscr{R}_{u_2} = 1-\xi^2$, $\mathscr{R}_{u_3} = (1-\xi^2)(1-\eta^2)$
Clamped (CCCC)	$\mathscr{R}_{u_1} = \mathscr{R}_{u_2} = \mathscr{R}_{u_3} = (1-\xi^2)(1-\eta^2)$

rewritten as

$$[\mathbf{K}_{11}^0 - \mathbf{K}_{13}^0(\mathbf{K}_{33}^0)^{-1}\mathbf{K}_{31}^0]\mathbf{A}^0 + [\mathbf{K}_{12}^0 - \mathbf{K}_{13}^0(\mathbf{K}_{33}^0)^{-1}\mathbf{K}_{32}^0]\mathbf{B}^0 = \mathbf{T}_1^0$$

$$[\mathbf{K}_{21}^0 - \mathbf{K}_{23}^0(\mathbf{K}_{33}^0)^{-1}\mathbf{K}_{31}^0]\mathbf{A}^0 + [\mathbf{K}_{22}^0 - \mathbf{K}_{23}^0(\mathbf{K}_{33}^0)^{-1}\mathbf{K}_{32}^0]\mathbf{B}^0 = \mathbf{T}_2^0 \tag{21}$$

Then the coefficients $\mathbf{A}^0$, $\mathbf{B}^0$, and $\mathbf{C}^0$ of initial deformation U_1^0, U_2^0, and U_3^0 can be obtained by solving Eq. (21). The initial state denoted by U_1^0, U_2^0, and U_3^0 is the new equilibrium position of the vibration of the plate. The corresponding initial thermal stresses σ_{11}^0 and σ_{22}^0 induced by the applied temperature field under the constrains of the boundary supports of the plate are obtained by virtue of strain–displacement relation:

$$\begin{aligned}\sigma_{11}^0 &= \frac{E}{1-v^2}(\varepsilon_{11}^0 - \alpha\Delta T) + \frac{Ev}{1-v^2}(\varepsilon_{22}^0 - \alpha\Delta T)\\ &= \frac{E}{1-v^2}\frac{2}{a}\frac{\partial U_1^0}{\partial \xi} + \frac{Ev}{1-v^2}\frac{2}{b}\frac{\partial U_2^0}{\partial \eta} - \frac{E}{1-v}\alpha\Delta T\end{aligned} \tag{22a}$$

$$\begin{aligned}\sigma_{22}^0 &= \frac{Ev}{1-v^2}(\varepsilon_{11}^0 - \alpha\Delta T) + \frac{E}{1-v^2}(\varepsilon_{22}^0 - \alpha\Delta T)\\ &= \frac{Ev}{1-v^2}\frac{2}{a}\frac{\partial U_1^0}{\partial \xi} + \frac{E}{1-v^2}\frac{2}{b}\frac{\partial U_2^0}{\partial \eta} - \frac{E}{1-v}\alpha\Delta T\end{aligned} \tag{22b}$$

In the variation of Lagrangian function $\mathscr{L}$:

$$\delta\mathscr{L} = \delta[\mathscr{K} - (\mathscr{U} + \mathscr{W})]\,\mathrm{d}t = 0 \tag{23}$$

where $L = \mathscr{K} - (\mathscr{U} + \mathscr{W})$ is the Lagrangian function; $\mathscr{K}$ is the total kinetic energy; $\mathscr{U}$ is the strain energy; $\mathscr{W}$ is the work done by the external forces.

In the present case, $\mathscr{W}$ is the work done by the initial thermal stresses σ_{11}^0 and σ_{22}^0:

$$\mathscr{W} = \int_V \left[\sigma_{11}^0 \frac{1}{2}\left(\frac{\partial \widetilde{U}_3}{\partial x_1}\right)^2 + \sigma_{22}^0 \frac{1}{2}\left(\frac{\partial \widetilde{U}_3}{\partial x_2}\right)^2\right] \mathrm{d}V \tag{24}$$

The strain energy is

$$\mathscr{U} = \frac{1}{2}\int_V (\sigma_{11}\varepsilon_{11} + \sigma_{22}\varepsilon_{22} + \sigma_{33}\varepsilon_{33} + 2\sigma_{23}\varepsilon_{23} + 2\sigma_{31}\varepsilon_{31} + 2\sigma_{12}\varepsilon_{12})\,\mathrm{d}V \tag{25}$$

The kinetic energy $\mathscr{K}$ is

$$\mathscr{K} = \int_V \frac{1}{2}\rho(\zeta)\left[\left(\frac{\partial u_1}{\partial t}\right)^2 + \left(\frac{\partial u_2}{\partial t}\right)^2 + \left(\frac{\partial u_3}{\partial t}\right)^2\right] \mathrm{d}V \tag{26}$$

in which the partial differential of the static deformation U_i^0 $(i = 1, 2, 3)$ with respect to t is zero. Therefore Eq. (26) is actually

$$\mathscr{K} = \int_V \frac{1}{2}\rho(\zeta)\left\{\left[\frac{\partial\left(\widetilde{U}_1 \mathrm{e}^{\mathrm{i}\omega t}\right)}{\partial t}\right]^2 + \left[\frac{\partial\left(\widetilde{U}_2 \mathrm{e}^{\mathrm{i}\omega t}\right)}{\partial t}\right]^2 + \left[\frac{\partial\left(\widetilde{U}_3 \mathrm{e}^{\mathrm{i}\omega t}\right)}{\partial t}\right]^2\right\} \mathrm{d}V \tag{27}$$

Based on Ritz method, substituting the work done by initial thermal stresses $\mathscr{W}$, the strain energy $\mathscr{U}$ and the kinetic energy $\mathscr{K}$ into the Lagrangian function, its partial differentials with respect to the coefficients $\widetilde{A}_{ijk}$, $\widetilde{B}_{lmn}$, and $\widetilde{C}_{pqr}$:

$$\frac{\partial\mathscr{L}}{\partial\widetilde{A}_{ijk}} = 0, \quad \frac{\partial\mathscr{L}}{\partial\widetilde{B}_{lmn}} = 0, \quad \frac{\partial\mathscr{L}}{\partial\widetilde{C}_{pqr}} = 0 \quad (i, j, k, l, m, n, p, q, r = 1, 2, 3, \ldots) \tag{28}$$

yield the following governing equations:

$$\hat{\mathbf{K}}_{11}\widetilde{\mathbf{A}} - \omega^2\mathbf{M}_{11}\widetilde{\mathbf{A}} + \hat{\mathbf{K}}_{12}\widetilde{\mathbf{B}} + \hat{\mathbf{K}}_{13}\widetilde{\mathbf{C}} = \mathbf{0}$$

$$\hat{\mathbf{K}}_{21}\widetilde{\mathbf{A}} + \hat{\mathbf{K}}_{22}\widetilde{\mathbf{B}} - \omega^2\mathbf{M}_{22}\widetilde{\mathbf{B}} + \hat{\mathbf{K}}_{23}\widetilde{\mathbf{C}} = \mathbf{0}$$

$$\hat{\mathbf{K}}_{31}\widetilde{\mathbf{A}} + \hat{\mathbf{K}}_{32}\widetilde{\mathbf{B}} + \hat{\mathbf{K}}_{33}\widetilde{\mathbf{C}} + (\mathbf{T}_{33|\xi} + \mathbf{T}_{33|\eta})\widetilde{\mathbf{C}} - \omega^2\mathbf{M}_{33}\widetilde{\mathbf{C}} = \mathbf{0} \tag{29}$$

which can be rewritten as standard eigenvalue matrix:

$$\left(\begin{bmatrix} \hat{\mathbf{K}}_{11} & \hat{\mathbf{K}}_{12} & \hat{\mathbf{K}}_{13} \\ & \hat{\mathbf{K}}_{22} & \hat{\mathbf{K}}_{23} \\ \text{Sym.} & & \hat{\mathbf{K}}_{33} + \mathbf{T}_{33|\xi} + \mathbf{T}_{33|\eta} \end{bmatrix} - \omega^2 \begin{bmatrix} \mathbf{M}_{11} & 0 & 0 \\ 0 & \mathbf{M}_{22} & 0 \\ 0 & 0 & \mathbf{M}_{33} \end{bmatrix} \right) \begin{Bmatrix} \widetilde{\mathbf{A}} \\ \widetilde{\mathbf{B}} \\ \widetilde{\mathbf{C}} \end{Bmatrix} = 0 \tag{30}$$

It is seen from Eq. (30) that the stiffness of the plate is affected by not only the temperature-dependent material properties but also the initial thermal stresses under the constrains of the boundary supports. The stiffness matrix elements $\hat{\mathbf{K}}_{ij}$ are dependent of temperature because of the temperature-dependent material properties. The additional thermal terms $\mathbf{T}_{33|\xi}$ and $\mathbf{T}_{33|\eta}$ modifying $\hat{\mathbf{K}}_{33}$ element are arisen because of the temperature rise under the constrains of the boundary supports. The compressive stresses, which develop when the temperature rises under the constrains of the boundary supports, will cause the initial deflection and hence reduce the stiffness of the plate. Eigenvectors $\widetilde{\mathbf{A}}$, $\widetilde{\mathbf{B}}$, and $\widetilde{\mathbf{C}}$ are the coefficients of the periodic displacements at the new equilibrium position. The respective elements in the nominal stiffness matrix $\mathbf{K}$ and mass matrix $\mathbf{M}$ are listed in details in Appendix A.

4. Verification

To verify the present approach, the numerical results of clamped Si_3N_4/SUS304 FGM square plates are compared with the published results in the literature in this subsection.

For simplicity, the non-dimensional natural frequency parameter is defined as

$$\omega = \frac{\omega b^2}{\pi^2}\sqrt{\frac{I_0}{D_0}} \tag{31}$$

where $I_0 = h\rho$, $D_0 = Eh^3/12(1-\nu^2)$. The material properties, ρ, E, and ν are chosen to be the values of stainless steel at the reference temperature $T_0 = 300\,\mathrm{K}$.

The numerical results of frequency parameters of the first eight modes of clamped Si_3N_4/SUS304 FGM square plates are compared with the results of other researchers [5,7] in Table 3. The square plates with thickness-side ratio $h/b = 0.1$ and volume fraction index $\kappa = 2$ are subjected to the different uniform temperature rises ($\Delta T = 0, 300, 500\,\mathrm{K}$). Table 3 shows a good agreement with those in Refs. [5,7].

Table 3
Comparisons of first eight natural frequency parameters for CCCC Si_3N_4/SUS304 FGM square plates subjected to uniform temperature rise ($a = 0.2\,\mathrm{m}$, $h/b = 0.1$, $\kappa = 2.0$, $T_0 = 300\,\mathrm{K}$).

ΔT (K)	Source	ω_1	ω_2 (ω_3)	ω_4	ω_5	ω_6	ω_7	ω_8
0	Yang [5]	4.1062	7.8902	11.1834	12.5881	13.1867	15.4530	16.0017
	Kim [7]	4.1165	7.9696	11.2198	13.1060	13.2089	15.9471	15.9471
	Present	4.1658	7.9389	11.1212	13.0973	13.2234	15.3627	15.3627
300	Yang [5]	3.6636	7.2544	10.3924	11.7054	12.3175	14.4520	15.0019
	Kim [7]	3.6593	7.3098	10.4021	12.1982	12.3052	14.9090	14.9090
	Present	3.7202	7.3010	10.3348	12.2256	12.3563	14.8112	14.8112
500	Yang [5]	3.2357	6.6281	9.5900	10.8285	11.4350	13.4412	13.9756
	Kim [7]	3.2147	6.6561	9.5761	11.2708	11.3812	13.8346	13.8346
	Present	3.2741	6.6509	9.5192	11.3126	11.4468	13.7907	13.7907

Table 4
Comparisons of first eight natural frequency parameters for CCCC Si_3N_4/SUS304 FGM rectangular plates subjected to uniform temperature rise ($a = 0.2\,m$, $h/b = 0.1$, $T_0 = 300\,K$, $\Delta T = 300\,K$).

a/b	κ	Source	ω_1	ω_2	ω_3	ω_4	ω_5	ω_6	ω_7	ω_8
0.5	2.0	Yang [5]	9.2196	11.6913	15.2957	20.4667	21.2323	21.4468	22.4853	25.4461
		Present	9.2111	11.5890	15.5999	19.9043	20.0234	20.7922	21.9073	25.0100
	10.0	Yang [5]	7.9839	10.1219	13.3088	17.6295	18.3727	18.9066	19.3778	21.9914
		Present	7.8170	9.8332	13.2410	16.8733	16.9943	17.6538	18.5960	21.2369
1.0	2.0	Yang [5]	3.6636	7.2544	7.2544	10.3924	11.7054	12.3175	14.4520	–
		Present	3.7202	7.3010	7.3010	10.3348	12.2256	12.3563	14.8112	14.8112
	10.0	Yang [5]	3.1835	6.3001	6.3001	9.0171	10.2372	10.6781	12.6015	12.9948
		Present	3.1398	6.1857	6.1857	8.7653	10.3727	10.4866	12.5971	12.5971
1.5	2.0	Yang [5]	2.7373	4.2236	6.6331	6.6331	7.9088	9.8122	10.0191	11.1492
		Present	2.7904	4.2839	6.6401	6.7227	7.8941	9.8528	9.9676	11.4179
	10.0	Yang [5]	2.3753	3.6692	5.7618	5.7618	6.8690	8.5206	8.6979	9.7598
		Present	2.3470	3.6147	5.6234	5.6910	6.6888	8.3553	8.4522	9.6859

Table 4 shows the comparisons of the first eight natural frequency parameters of clamped Si_3N_4/SUS304 FGM rectangular plates with the solutions of Yang and Shen [5]. The plates subjected to the uniform temperature rise ($\Delta T = 300\,K$) are of thickness-side ratio $h/b = 0.1$, different aspect ratios ($a/b = 0.5, 1.0, 1.5$) and volume fraction index ($\kappa = 2, 10$). They also show that the present results agree well with those of Yang and Shen [5].

5. Parametric study

Based on the procedures and analyses of foregoing sections, the simply supported and clamped Si_3N_4/SUS304 FGM rectangular plates are investigated. In the succedent computation, $12 \times 12 \times 6$ terms of admissible functions (U_i^0 and $\widetilde{U}_i$, $i = 1, 2, 3$) for each displacement function are used.

Tables 5–7 give the results of the first seven natural frequency parameters of the simply supported case. Tables 8–10 give the results of the first seven natural frequency parameters of the clamped case. Three temperature fields: uniform temperature rise, linear temperature rise, and nonlinear temperature rise, as defined previously in Eqs. (2), (3), and (5), are considered. These results include the cases of three thickness-side ratios ($h/b = 0.05, 0.1, 0.2$), two aspect ratios ($a/b = 0.5, 1.0$) and four volume fraction indices ($\kappa = 1.0, 2.0, 5.0, 10.0$). It is shown that for both simply supported and clamped plates, the natural frequency parameters decrease with the increase of the volume fraction index κ.

Figs. 2 and 3 display the first four frequency parameters ω_i ($i = 1, 2, 3, 4$) versus temperature for simply supported and clamped square Si_3N_4/SUS304 FGM plates of thickness-side ratio $h/b = 0.1$, respectively. The plates of two volume fraction indices ($\kappa = 1, 10$) subjected to uniform, linear, and nonlinear temperature rise fields are considered. For the purpose of comparison of temperature effects, the data of first natural frequency parameters ω_1 from Figs. 2 and 3 are plotted in Fig. 4. The curves are displayed as four sets. Obviously, the temperature effects of vibrational frequencies of clamped plates are greater than those of simply supported plates. Because the thermal stresses induced by the temperature rise along the supported edges can fully develop when the edges of plates are fully constrained i.e. the clamped support condition. The uniform temperature change affects the vibrational frequencies more significantly than the linear and nonlinear temperature changes. It can be explained by referring to Fig. 1 which is shown that the temperature variation of the uniform temperature field is more intensive than those of linear and nonlinear temperature fields.

For a clear demonstration, Tables 11 and 12 list the reduction ratios (%) of frequency parameters due to the temperature rises. The temperatures of plates are raised from the initial value 300 K to the final value 800 K. It

Table 5
Natural frequency parameters for SSSS rectangular Si_3N_4/SUS304 FGM plates subjected to uniform temperature rise $\Delta T = 300\,K$.

h/b	a/b	κ	ω_1	ω_2	ω_3	ω_4	ω_5	ω_6	ω_7
0.05	0.5	1.0	6.4596	10.0710	16.1651	17.5313	21.4332	24.4401	24.7910
		2.0	5.7463	8.9452	14.3663	15.4507	19.1018	21.7343	22.0788
		5.0	5.1762	8.0455	12.9257	13.7556	17.2278	19.5618	19.8982
		10.0	4.8947	7.6045	12.2218	12.9823	16.3079	18.5046	18.8320
	1.0	1.0	2.3527	6.2312	6.2312	10.0141	12.5913	12.6199	16.2332
		2.0	2.0674	5.5220	5.5220	8.8894	11.1928	11.2210	14.4335
		5.0	1.8415	4.9565	4.9565	7.9908	10.0729	10.1004	12.9910
		10.0	1.7328	4.6798	4.6798	7.5508	9.5234	9.5500	12.2850
0.1	0.5	1.0	6.2330	8.7623	9.5264	14.5811	17.4976	17.4976	18.4210
		2.0	5.5543	7.7231	8.4816	12.9754	15.4288	15.4288	16.4012
		5.0	5.0084	6.8769	7.6398	11.6782	13.7470	13.7470	14.7653
		10.0	4.7408	6.4908	7.2322	11.0596	12.9790	12.9790	13.9905
	1.0	1.0	2.5511	6.1761	6.1761	8.7623	8.7623	9.5119	11.6301
		2.0	2.2690	5.4984	5.4984	7.7231	7.7231	8.4675	10.3536
		5.0	2.0433	4.9538	4.9538	6.8769	6.8769	7.6257	9.3240
		10.0	1.9323	4.6881	4.6881	6.4908	6.4908	7.2191	8.8282
0.2	0.5	1.0	4.3744	5.2586	7.5826	8.6967	8.6967	9.7045	10.7982
		2.0	3.8572	4.6809	6.7428	7.6806	7.6806	8.5751	9.5965
		5.0	3.4368	4.2124	6.0617	6.8603	6.8603	7.6653	8.6236
		10.0	3.2447	3.9922	5.7484	6.4843	6.4843	7.2478	8.1871
	1.0	1.0	2.3902	4.3744	4.3744	5.2423	5.2423	6.1738	7.5780
		2.0	2.1289	3.8572	3.8572	4.6648	4.6648	5.4468	6.7384
		5.0	1.9182	3.4368	3.4368	4.1967	4.1967	4.8571	6.0573
		10.0	1.8160	3.2447	3.2447	3.9768	3.9768	4.5875	5.7440

Table 6
Natural frequency parameters for SSSS rectangular Si_3N_4/SUS304 FGM plates subjected to linear temperature rise $\Delta T = 300\,K$.

h/b	a/b	κ	ω_1	ω_2	ω_3	ω_4	ω_5	ω_6	ω_7
0.05	0.5	1.0	6.7201	10.5613	16.8720	17.9366	21.9850	25.3695	25.5166
		2.0	5.9985	9.4202	15.0505	15.8531	19.6341	22.6331	22.7793
		5.0	5.4203	8.5033	13.5879	14.1543	17.7548	20.4371	20.5878
		10.0	5.1808	8.1238	12.9796	13.4404	16.9666	19.5186	19.6685
	1.0	1.0	2.6173	6.6264	6.6264	10.5380	13.1379	13.1499	16.9005
		2.0	2.3252	5.9048	5.9048	9.3967	11.7208	11.7324	15.0783
		5.0	2.0880	5.3237	5.3237	8.4790	10.5842	10.5963	13.6166
		10.0	1.9917	5.0845	5.0845	8.0994	10.1121	10.1240	13.0080
0.1	0.5	1.0	6.3941	8.9648	9.7960	14.9815	17.9021	17.9021	18.8299
		2.0	5.7220	7.9243	8.7561	13.3847	15.8307	15.8307	16.8593
		5.0	5.1621	7.0763	7.8973	12.0640	14.1456	14.1456	15.1664
		10.0	4.9323	6.7198	7.5410	11.5124	13.4367	13.4367	14.4698
	1.0	1.0	2.6543	6.3702	6.3702	8.9648	8.9648	9.7899	11.9453
		2.0	2.3688	5.6858	5.6858	7.9243	7.9243	8.7359	10.6584
		5.0	2.1399	5.1376	5.1376	7.0763	7.0763	7.8909	9.6266
		10.0	2.0450	4.9078	4.9078	6.7198	6.7198	7.5346	9.1900
0.2	0.5	1.0	4.4755	5.3755	7.7590	8.8978	8.8978	9.9290	11.0495
		2.0	3.9577	4.7945	6.9156	7.8808	7.8808	8.7987	9.8448
		5.0	3.5364	4.3277	6.2376	7.0593	7.0593	7.8877	8.8789
		10.0	3.3592	4.1280	5.9453	6.7125	6.7125	7.5027	8.4580
	1.0	1.0	2.4526	4.4755	4.4755	5.3688	5.3688	6.3166	7.7572
		2.0	2.1893	3.9577	3.9577	4.7877	4.7877	5.5887	6.9138
		5.0	1.9780	3.5364	3.5364	4.3205	4.3205	4.9980	6.2356
		10.0	1.8890	3.3592	3.3592	4.1209	4.1209	4.7492	5.9434

Table 7
Natural frequency parameters for SSSS rectangular Si_3N_4/SUS304 FGM plates subjected to nonlinear temperature rise $\Delta T = 300\,K$.

h/b	a/b	κ	ω_1	ω_2	ω_3	ω_4	ω_5	ω_6	ω_7
0.05	0.5	1.0	6.7286	10.5780	16.8958	17.9485	22.0016	25.4005	25.5394
		2.0	6.0084	9.4391	15.0779	15.8647	19.6554	22.6694	22.8074
		5.0	5.4269	8.5165	13.6064	14.1632	17.7661	20.4604	20.6038
		10.0	5.1848	8.1313	12.9904	13.4467	16.9746	19.5326	19.6791
	1.0	1.0	2.6263	6.6395	6.6395	10.5555	13.1555	13.1667	16.9223
		2.0	2.3306	5.9149	5.9149	9.4129	11.7364	11.7494	15.1006
		5.0	2.0957	5.3344	5.3344	8.4929	10.5979	10.6092	13.6333
		10.0	1.9959	5.0907	5.0907	8.1075	10.1205	10.1321	13.0181
0.1	0.5	1.0	6.3989	8.9707	9.8048	14.9954	17.9138	17.9138	18.8444
		2.0	5.7159	7.9300	8.7527	13.3792	15.8419	15.8419	16.8140
		5.0	5.1655	7.0806	7.9031	12.0724	14.1532	14.1532	15.1738
		10.0	4.9343	6.7230	7.5447	11.5179	13.4430	13.4430	14.4757
	1.0	1.0	2.6576	6.3764	6.3764	8.9707	8.9707	9.7992	11.9555
		2.0	2.3727	5.6933	5.6933	7.9300	7.9300	8.7468	10.6709
		5.0	2.1424	5.1419	5.1419	7.0806	7.0806	7.8970	9.6331
		10.0	2.0465	4.9106	4.9106	6.7230	6.7230	7.5386	9.1945
0.2	0.5	1.0	4.4785	5.3798	7.7663	8.9034	8.9034	9.9351	11.0597
		2.0	3.9605	4.7991	6.9230	7.8860	7.8860	8.8044	9.8563
		5.0	3.5383	4.3296	6.2404	7.0612	7.0612	7.8891	8.8821
		10.0	3.3608	4.1294	5.9475	6.7157	6.7157	7.5063	8.4611
	1.0	1.0	2.4546	4.4785	4.4785	5.3734	5.3734	6.3206	7.7644
		2.0	2.1916	3.9605	3.9605	4.7926	4.7926	5.5926	6.9213
		5.0	1.9793	3.5383	3.5383	4.3229	4.3229	5.0002	6.2386
		10.0	1.8893	3.3608	3.3608	4.1224	4.1224	4.7514	5.9454

Table 8
Natural frequency parameters for CCCC rectangular Si_3N_4/SUS304 FGM plates subjected to uniform temperature rise $\Delta T = 300\,K$.

h/b	a/b	κ	ω_1	ω_2	ω_3	ω_4	ω_5	ω_6	ω_7
0.05	0.5	1.0	11.5387	14.8354	20.8074	29.1040	29.1079	32.0641	37.1140
		2.0	10.1650	13.0787	18.3834	25.7642	25.7695	28.3955	32.8795
		5.0	9.0661	11.6718	16.4382	23.0751	23.0861	25.4414	29.4664
		10.0	8.5436	11.0033	15.5135	21.7992	21.8220	24.0507	27.8614
	1.0	1.0	3.5231	8.2404	8.2404	12.5066	15.3498	15.4874	19.2707
		2.0	2.9708	7.1830	7.1830	10.9833	13.5177	13.6451	17.0079
		5.0	2.5282	6.3396	6.3396	9.7655	12.0511	12.1705	15.1937
		10.0	2.3247	5.9413	5.9413	9.1865	11.3525	11.4671	14.3290
0.1	0.5	1.0	10.3932	13.0762	17.5982	22.4803	22.6024	23.4556	24.7253
		2.0	9.2111	11.5890	15.5999	19.9043	20.0234	20.7922	21.9073
		5.0	8.2568	10.3868	13.9819	17.8183	17.9309	18.6333	19.6207
		10.0	7.8170	9.8332	13.2410	16.8733	16.9943	17.6538	18.5960
	1.0	1.0	4.2110	8.2429	8.2429	11.6602	13.7916	13.9366	16.6856
		2.0	3.7202	7.3010	7.3010	10.3348	12.2256	12.3563	14.8112
		5.0	3.3267	6.5424	6.5424	9.2647	10.9594	11.0790	13.2936
		10.0	3.1398	6.1857	6.1857	8.7653	10.3727	10.4866	12.5971
0.2	0.5	1.0	7.2986	9.0576	11.1478	11.7768	13.8548	14.8097	15.0543
		2.0	6.4571	8.0189	9.8922	10.4335	12.3109	13.1850	13.3496
		5.0	5.7749	7.1768	8.8890	9.3471	11.0516	11.9219	11.9801
		10.0	5.4780	6.8089	8.4344	8.8741	10.5014	11.3665	11.3876
	1.0	1.0	3.5998	6.3100	6.3100	8.3190	8.3190	8.4858	9.6721
		2.0	3.1905	5.5903	5.5903	7.3936	7.3936	7.5185	8.5707
		5.0	2.8595	5.0064	5.0064	6.6503	6.6503	6.7339	7.6772
		10.0	2.7084	4.7455	4.7455	6.3168	6.3168	6.3862	7.2835

Table 9
Natural frequency parameters for CCCC rectangular Si_3N_4/SUS304 FGM plates subjected to linear temperature rise $\Delta T = 300\,K$.

h/b	a/b	κ	ω_1	ω_2	ω_3	ω_4	ω_5	ω_6	ω_7
0.05	0.5	1.0	12.4535	15.9486	22.1325	30.5466	30.6611	33.6119	38.8182
		2.0	11.0699	14.1787	19.6892	27.1841	27.2905	29.9130	34.5495
		5.0	9.9476	12.7439	17.7126	24.4732	24.5691	26.9308	31.1081
		10.0	9.4849	12.1505	16.8910	23.3376	23.4312	25.6796	29.6610
	1.0	1.0	4.4447	9.3057	9.3057	13.6919	16.5979	16.7187	20.6198
		2.0	3.9120	8.2474	8.2474	12.1599	14.7531	14.8629	18.3398
		5.0	3.4649	7.3791	7.3791	10.9119	13.2546	13.3564	16.4923
		10.0	3.2862	7.0252	7.0252	10.3988	12.6360	12.7344	15.7263
0.1	0.5	1.0	10.7833	13.5614	18.2101	22.9658	23.3196	24.2168	25.5033
		2.0	9.5908	12.0620	16.1971	20.3837	20.7212	21.5365	22.6654
		5.0	8.6327	10.8560	14.5770	18.2919	18.6326	19.3795	20.3836
		10.0	8.2279	10.3448	13.8868	17.4155	17.7359	18.4552	19.4027
	1.0	1.0	4.4806	8.6303	8.6303	12.1387	14.3219	14.4644	17.0322
		2.0	3.9858	7.6806	7.6806	10.8028	12.7439	12.8721	15.1513
		5.0	3.5858	6.9152	6.9152	9.7268	11.4729	11.5900	13.6269
		10.0	3.4199	6.5939	6.5939	9.2722	10.9339	11.0466	12.9907
0.2	0.5	1.0	7.5087	9.3186	11.3891	12.1099	14.2242	15.1259	15.4736
		2.0	6.6602	8.2727	10.1309	10.7594	12.6762	13.4875	13.7618
		5.0	5.9808	7.4349	9.1253	9.6800	11.4333	12.2146	12.4033
		10.0	5.6878	7.0712	8.7025	9.2068	10.8780	11.6837	11.7989
	1.0	1.0	3.7236	6.5061	6.5061	8.4882	8.4882	8.7378	9.9545
		2.0	3.3109	5.7813	5.7813	7.5600	7.5600	7.7648	8.8469
		5.0	2.9794	5.1988	5.1988	6.8144	6.8144	6.9834	7.9580
		10.0	2.8386	4.9484	4.9484	6.5029	6.5029	6.6450	7.5710

Table 10
Natural frequency parameters for CCCC rectangular Si_3N_4/SUS304 FGM plates subjected to nonlinear temperature rise $\Delta T = 300\,K$.

h/b	a/b	κ	ω_1	ω_2	ω_3	ω_4	ω_5	ω_6	ω_7
0.05	0.5	1.0	12.4872	15.9895	22.1809	30.5986	30.7175	33.6677	38.8797
		2.0	11.1064	14.2231	19.7421	27.2418	27.3525	29.9749	34.6176
		5.0	9.9766	12.7789	17.7532	24.5155	24.6150	26.9758	31.1569
		10.0	9.5000	12.1689	16.9128	23.3612	23.4566	25.7049	29.6887
	1.0	1.0	4.4780	9.3453	9.3453	13.7358	16.6440	16.7641	20.6694
		2.0	3.9471	8.2896	8.2896	12.2071	14.8029	14.9121	18.3936
		5.0	3.4954	7.4142	7.4142	10.9500	13.2942	13.3953	16.5341
		10.0	3.3011	7.0428	7.0428	10.4184	12.6567	12.7547	15.7485
0.1	0.5	1.0	10.7970	13.5788	18.2325	22.9807	23.3455	24.2450	25.5317
		2.0	9.6065	12.0816	16.2221	20.3972	20.7512	21.5683	22.6981
		5.0	8.6437	10.8693	14.5931	18.2998	18.6509	19.3985	20.4029
		10.0	8.2343	10.3527	13.8965	17.4229	17.7475	18.4671	19.4151
	1.0	1.0	4.4904	8.6443	8.6443	12.1559	14.3412	14.4836	17.0433
		2.0	3.9965	7.6961	7.6961	10.8220	12.7653	12.8934	15.1611
		5.0	3.5941	6.9264	6.9264	9.7400	11.4873	11.6043	13.6331
		10.0	3.4243	6.6002	6.6002	9.2799	10.9425	11.0551	12.9958
0.2	0.5	1.0	7.5155	9.3271	11.3954	12.1195	14.2342	15.1267	15.4810
		2.0	6.6691	8.2841	10.1369	10.7745	12.6930	13.4958	13.7818
		5.0	5.9862	7.4408	9.1258	9.6862	11.4383	12.2128	12.4090
		10.0	5.6915	7.0757	8.7064	9.2126	10.8850	11.6899	11.8070
	1.0	1.0	3.7280	6.5132	6.5132	8.4932	8.4932	8.7469	9.9641
		2.0	3.3159	5.7896	5.7896	7.5646	7.5646	7.7758	8.8594
		5.0	2.9827	5.2037	5.2037	6.8161	6.8161	6.9890	7.9640
		10.0	2.8406	4.9515	4.9515	6.5055	6.5055	6.6490	7.5755

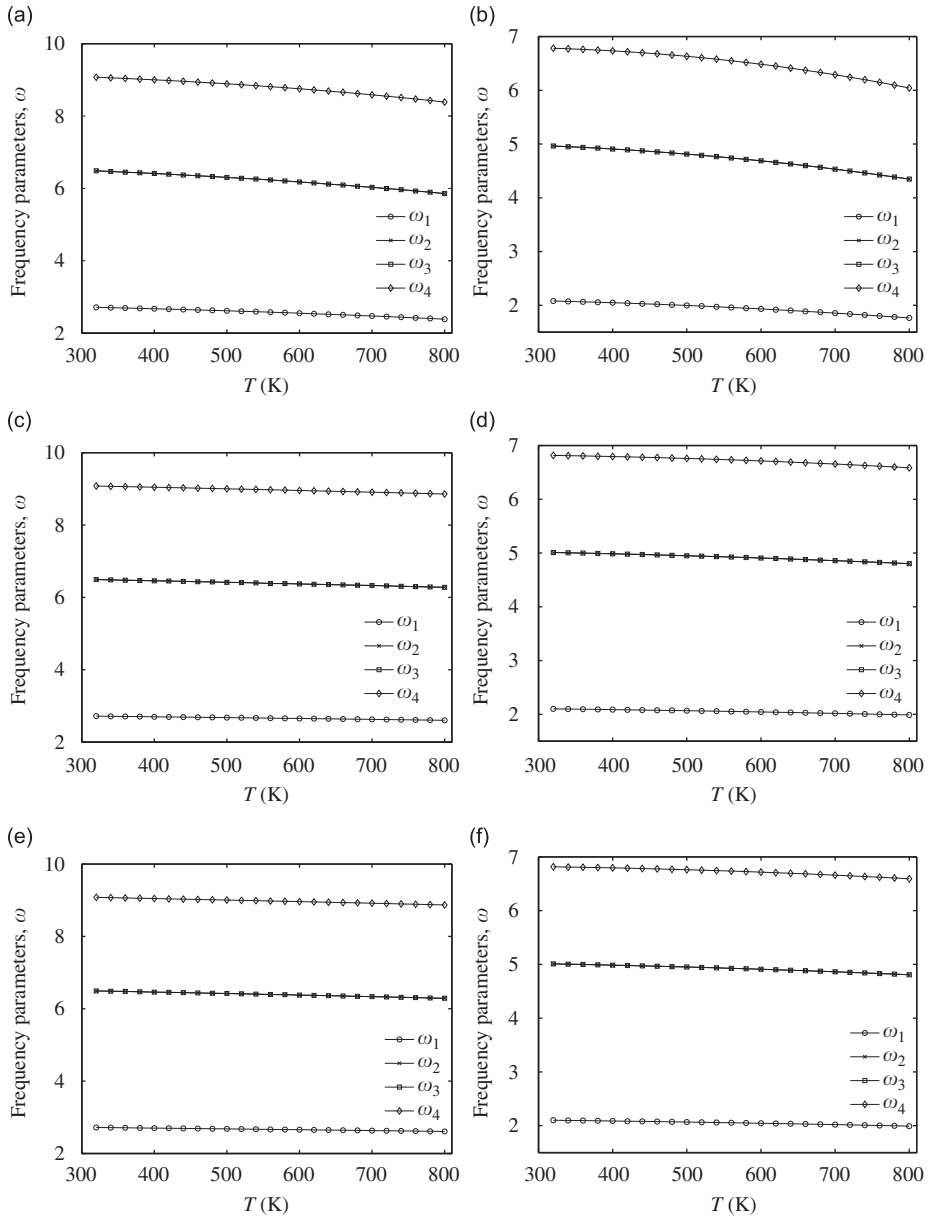

Fig. 2. First four frequency parameters ω_i versus temperature for SSSS square Si_3N_4/SUS304 FGM plates ($h/b = 0.1$): (a) uniform temperature field, $\kappa = 1$; (b) uniform temperature field, $\kappa = 10$; (c) linear temperature field, $\kappa = 1$; (d) linear temperature field, $\kappa = 10$; (e) nonlinear temperature field, $\kappa = 1$; (f) nonlinear temperature field, $\kappa = 10$.

is shown that the temperature rise affects the first mode more significantly than other higher modes. And the plates of volume fraction index $\kappa = 10$ are more sensitive to the temperature change than those of $\kappa = 1$.

6. Conclusion

Three-dimensional vibration analysis of power-law FGM rectangular plates has been carried out based on the linear, small strain three-dimensional elasticity theory via Ritz method. The simply supported and clamped FGM plates subjected to uniform temperature field, linear temperature field and nonlinear temperature field are considered. The accuracy of the present approach is validated by comparing the numerical results of

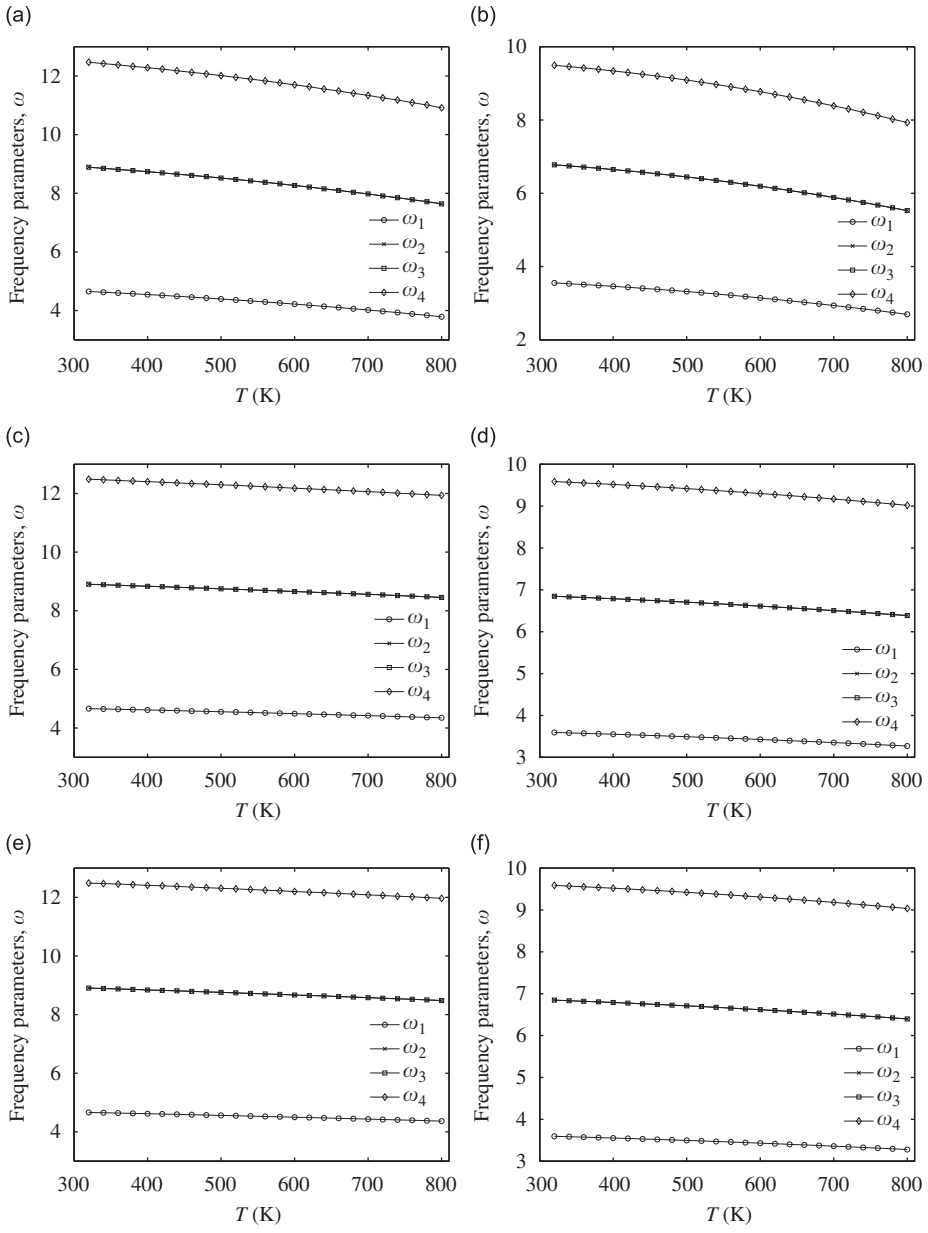

Fig. 3. First four frequency parameters ω_i versus temperature for CCCC square Si_3N_4/SUS304 FGM plates ($h/b = 0.1$): (a) uniform temperature field, $\kappa = 1$; (b) uniform temperature field, $\kappa = 10$; (c) linear temperature field, $\kappa = 1$; (d) linear temperature field, $\kappa = 10$; (e) nonlinear temperature field, $\kappa = 1$; (f) nonlinear temperature field, $\kappa = 10$.

clamped plates with the results of other researchers. Parametric study for supported conditions, temperature fields, volume fraction indices shows that:

(1) the temperature effects on vibrational frequencies of clamped plates are greater than those of simply supported plates;
(2) the uniform temperature change affects the vibrational frequencies more significantly than the linear and nonlinear temperature changes;
(3) the temperature change affects the first mode more significantly than other higher modes;
(4) the plates of volume fraction $\kappa = 10$ are more sensitive to the temperature change than those of $\kappa = 1$.

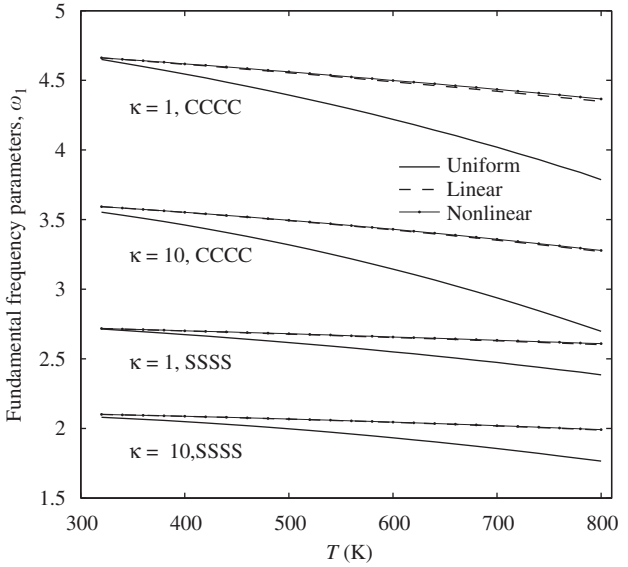

Fig. 4. The natural fundamental frequency parameters ω_1 versus temperature for square Si_3N_4/SUS304 FGM plates ($h/b = 0.1$).

Table 11
Temperature effects of frequency parameters of SSSS square Si_3N_4/SUS304 FGM plates ($h/b = 0.1$).

κ	Temp.	ω_1			ω_2 (ω_3)			ω_4		
		300 K	800 K	Reduc. (%)	300 K	800 K	Reduc. (%)	300 K	800 K	Reduc. (%)
1	Uniform	2.7222	2.3850	12.39	6.5000	5.8561	9.91	9.0873	8.3872	7.70
	Linear	2.7222	2.6020	4.41	6.5000	6.2782	3.41	9.0873	8.8581	2.52
	Nonlinear	2.7222	2.6088	4.17	6.5000	6.2900	3.23	9.0873	8.8696	2.40
10	Uniform	2.0867	1.7654	15.39	4.9743	4.3482	12.59	6.7893	6.0424	11.00
	Linear	2.0867	1.9884	4.71	4.9743	4.8020	3.46	6.7893	6.5851	3.01
	Nonlinear	2.0867	1.9914	4.56	4.9743	4.8079	3.34	6.7893	6.5928	2.89

Table 12
Temperature effects of frequency parameters of CCCC square Si_3N_4/SUS304 FGM plates ($h/b = 0.1$).

κ	Temp.	ω_1			ω_2 (ω_3)			ω_4		
		300 K	800 K	Reduc. (%)	300 K	800 K	Reduc. (%)	300 K	800 K	Reduc. (%)
1	Uniform	4.6728	3.7869	18.96	8.9194	7.6393	14.35	12.5069	10.9168	12.71
	Linear	4.6728	4.3486	6.94	8.9194	8.4559	5.20	12.5069	11.9364	4.56
	Nonlinear	4.6728	4.3664	6.56	8.9194	8.4805	4.92	12.5069	11.9662	4.32
10	Uniform	3.5732	2.6979	24.50	6.8030	5.5295	18.72	9.5250	7.9307	16.74
	Linear	3.5732	3.2698	8.49	6.8030	6.3845	6.15	9.5250	9.0181	5.32
	Nonlinear	3.5732	3.2785	8.25	6.8030	6.3971	5.97	9.5250	9.0340	5.15

Acknowledgment

The financial support from the Research Committee of University of Macau is gratefully acknowledged (Grant no: RG049/06-07S/IVP/FST).

Appendix A. Elements of submatrices

The elements of the nominal stiffness submatrices **K** and mass submatrices **M** are listed below:

$$\hat{\mathbf{K}}_{11}=\frac{bh}{2a}K^{1,1}_{\xi,u_1iu_1\bar{i}}K^{0,0}_{\eta,u_1ju_1\bar{j}}(\hat{E}^{0,0}_{\lambda,k\bar{k}}+2\hat{E}^{0,0}_{\mu,k\bar{k}})+\frac{ah}{2b}K^{0,0}_{\xi,u_1iu_1\bar{i}}K^{1,1}_{\eta,u_1ju_1\bar{j}}\hat{E}^{0,0}_{\mu,k\bar{k}}+\frac{ab}{2h}K^{0,0}_{\xi,u_1iu_1\bar{i}}K^{0,0}_{\eta,u_1ju_1\bar{j}}\hat{E}^{1,1}_{\mu,k\bar{k}} \tag{A.1a}$$

$$\hat{\mathbf{K}}_{12}=\frac{h}{2}K^{1,0}_{\xi,u_1iu_2l}K^{0,1}_{\eta,u_1ju_2m}\hat{E}^{0,0}_{\lambda,kn}+\frac{h}{2}K^{0,1}_{\xi,u_1iu_2l}K^{1,0}_{\eta,u_1ju_2m}\hat{E}^{0,0}_{\mu,kn} \tag{A.1b}$$

$$\hat{\mathbf{K}}_{13}=\frac{b}{2}K^{1,0}_{\xi,u_1iu_3p}K^{0,0}_{\eta,u_1ju_3q}\hat{E}^{0,1}_{\lambda,kr}+\frac{b}{2}K^{0,1}_{\xi,u_1iu_3p}K^{0,0}_{\eta,u_1ju_3q}\hat{E}^{1,0}_{\mu,kr} \tag{A.1c}$$

$$\hat{\mathbf{K}}_{22}=\frac{ah}{2b}K^{0,0}_{\xi,u_2lu_2\bar{l}}K^{1,1}_{\eta,u_2mu_2\bar{m}}(\hat{E}^{0,0}_{\lambda,n\bar{n}}+2\hat{E}^{0,0}_{\mu,n\bar{n}})+\frac{ab}{2h}K^{0,0}_{\xi,u_2lu_2\bar{l}}K^{0,0}_{\eta,u_2mu_2\bar{m}}\hat{E}^{1,1}_{\mu,n\bar{n}}+\frac{bh}{2a}K^{1,1}_{\xi,u_2lu_2\bar{l}}K^{0,0}_{\eta,u_2mu_2\bar{m}}\hat{E}^{0,0}_{\mu,n\bar{n}} \tag{A.1d}$$

$$\hat{\mathbf{K}}_{23}=\frac{a}{2}K^{0,0}_{\xi,u_2lu_3p}K^{1,0}_{\eta,u_2mu_3q}\hat{E}^{0,1}_{\lambda,nr}+\frac{a}{2}K^{0,0}_{\xi,u_2lu_3p}K^{0,1}_{\eta,u_2mu_3q}\hat{E}^{1,0}_{\mu,nr} \tag{A.1e}$$

$$\hat{\mathbf{K}}_{33}=\frac{ab}{2h}K^{0,0}_{\xi,u_3pu_3\bar{p}}K^{0,0}_{\eta,u_3qu_3\bar{q}}(\hat{E}^{1,1}_{\lambda,r\bar{r}}+2\hat{E}^{1,1}_{\mu,r\bar{r}})+\frac{bh}{2a}K^{1,1}_{\xi,u_3pu_3\bar{p}}K^{0,0}_{\eta,u_3qu_3\bar{q}}\hat{E}^{0,0}_{\mu,r\bar{r}}+\frac{ah}{2b}K^{0,0}_{\xi,u_3pu_3\bar{p}}K^{1,1}_{\eta,u_3qu_3\bar{q}}\hat{E}^{0,0}_{\mu,r\bar{r}} \tag{A.1f}$$

$$\mathbf{M}_{11}=\frac{abh}{8}K^{0,0}_{\xi,u_1iu_1\bar{i}}K^{0,0}_{\eta,u_1ju_1\bar{j}}M_{\zeta,k\bar{k}} \tag{A.2a}$$

$$\mathbf{M}_{22}=\frac{abh}{8}K^{0,0}_{\xi,u_2lu_2\bar{l}}K^{0,0}_{\eta,u_2mu_2\bar{m}}M_{\zeta,n\bar{n}} \tag{A.2b}$$

$$\mathbf{M}_{33}=\frac{abh}{8}K^{0,0}_{\xi,u_3pu_3\bar{p}}K^{0,0}_{\eta,u_3qu_3\bar{q}}M_{\zeta,r\bar{r}} \tag{A.2c}$$

The additional thermal terms $\mathbf{T}_{33|\xi}$ and $\mathbf{T}_{33|\eta}$ are the thermal effects imposed by the initially thermal stresses σ^0_{11} and σ^0_{22}, respectively, which are shown below:

$$\begin{aligned}\mathbf{T}_{33|\xi}=&\frac{bh}{a^2}\sum_{i=1}^{\infty}\sum_{j=1}^{\infty}\sum_{k=1}^{\infty}A^0_{ijk}K^{1,1,1}_{\xi,u_1iu_3pu_3\bar{p}}K^{0,0,0}_{\eta,u_1ju_3qu_3\bar{q}}\hat{E}^{0,0,0}_{\zeta_1,kr\bar{r}}\\&+\frac{h}{a}\sum_{l=1}^{\infty}\sum_{m=1}^{\infty}\sum_{n=1}^{\infty}B^0_{lmn}K^{0,1,1}_{\xi,u_2lu_3pu_3\bar{p}}K^{1,0,0}_{\eta,u_2mu_3qu_3\bar{q}}\hat{E}^{0,0,0}_{\zeta_2,nr\bar{r}}\\&-\frac{bh}{2a}K^{1,1}_{\xi,u_3pu_3\bar{p}}K^{0,0}_{\eta,u_3qu_3\bar{q}}T_{\zeta,r\bar{r}}\end{aligned} \tag{A.3a}$$

$$\begin{aligned}\mathbf{T}_{33|\eta}=&\frac{h}{b}\sum_{i=1}^{\infty}\sum_{j=1}^{\infty}\sum_{k=1}^{\infty}A^0_{ijk}K^{1,0,0}_{\xi,u_1iu_3pu_3\bar{p}}K^{0,1,1}_{\eta,u_1ju_3qu_3\bar{q}}\hat{E}^{0,0,0}_{\zeta_2,kr\bar{r}}\\&+\frac{ah}{b^2}\sum_{l=1}^{\infty}\sum_{m=1}^{\infty}\sum_{n=1}^{\infty}B^0_{lmn}K^{0,0,0}_{\xi,u_2lu_3pu_3\bar{p}}K^{1,1,1}_{\eta,u_2mu_3qu_3\bar{q}}\hat{E}^{0,0,0}_{\zeta_1,nr\bar{r}}\\&-\frac{ah}{2b}K^{0,0}_{\xi,u_3pu_3\bar{p}}K^{1,1}_{\eta,u_3qu_3\bar{q}}T_{\zeta,r\bar{r}}\end{aligned} \tag{A.3b}$$

For the describable convenience, the operators K_ξ, K_η, E_λ, E_μ, and M_ζ are used in above equations and defined as

$$K^{s_1,s_2,s_3}_{\xi,\beta_1\varphi_1\beta_2\varphi_2\beta_3\varphi_3}=\int_{-1}^{1}\frac{\mathrm{d}^{s_1}[f^{(1)}_{\beta_1}(\xi)P_{\varphi_1}(\xi)]}{\mathrm{d}\xi^{s_1}}\cdot\frac{\mathrm{d}^{s_2}[f^{(1)}_{\beta_2}(\xi)P_{\varphi_2}(\xi)]}{\mathrm{d}\xi^{s_2}}\cdot\frac{\mathrm{d}^{s_3}[f^{(1)}_{\beta_3}(\xi)P_{\varphi_3}(\xi)]}{\mathrm{d}\xi^{s_3}}\,\mathrm{d}\xi \tag{A.4a}$$

$$K^{s_1,s_2,s_3}_{\eta,\beta_1\varphi_1\beta_2\varphi_2\beta_3\varphi_3} = \int_{-1}^{1} \frac{\mathrm{d}^{s_1}[f^{(2)}_{\beta_1}(\eta)P_{\varphi_1}(\eta)]}{\mathrm{d}\eta^{s_1}} \cdot \frac{\mathrm{d}^{s_2}[f^{(2)}_{\beta_2}(\eta)P_{\varphi_2}(\eta)]}{\mathrm{d}\eta^{s_2}} \cdot \frac{\mathrm{d}^{s_3}[f^{(2)}_{\beta_3}(\eta)P_{\varphi_3}(\eta)]}{\mathrm{d}\eta^{s_3}}\,\mathrm{d}\eta \tag{A.4b}$$

$$K^{s_1,s_2}_{\xi,\beta_1\varphi_1\beta_2\varphi_2} = \int_{-1}^{1} \frac{\mathrm{d}^{s_1}[f^{(1)}_{\beta_1}(\xi)P_{\varphi_1}(\xi)]}{\mathrm{d}\xi^{s_1}} \cdot \frac{\mathrm{d}^{s_2}[f^{(1)}_{\beta_2}(\xi)P_{\varphi_2}(\xi)]}{\mathrm{d}\xi^{s_2}}\,\mathrm{d}\xi \tag{A.4c}$$

$$K^{s_1,s_2}_{\eta,\beta_1\varphi_1\beta_2\varphi_2} = \int_{-1}^{1} \frac{\mathrm{d}^{s_1}[f^{(2)}_{\beta_1}(\eta)P_{\varphi_1}(\eta)]}{\mathrm{d}\eta^{s_1}} \cdot \frac{\mathrm{d}^{s_2}[f^{(2)}_{\beta_2}(\eta)P_{\varphi_2}(\eta)]}{\mathrm{d}\eta^{s_2}}\,\mathrm{d}\eta \tag{A.4d}$$

$$\hat{E}^{s_1,s_2,s_3}_{\zeta_1,\varphi_1\varphi_2\varphi_3} = \int_{-1}^{1} \frac{E(\zeta,T)}{1-v^2(\zeta,T)} \cdot \frac{\mathrm{d}^{s_1}P_{\varphi_1}(\zeta)}{\mathrm{d}\zeta^{s_1}} \cdot \frac{\mathrm{d}^{s_2}P_{\varphi_2}(\zeta)}{\mathrm{d}\zeta^{s_2}} \cdot \frac{\mathrm{d}^{s_3}P_{\varphi_3}(\zeta)}{\mathrm{d}\zeta^{s_3}}\,\mathrm{d}\zeta \tag{A.5a}$$

$$\hat{E}^{s_1,s_2,s_3}_{\zeta_2,\varphi_1\varphi_2\varphi_3} = \int_{-1}^{1} \frac{E(\zeta,T)v(\zeta,T)}{1-v^2(\zeta,T)} \cdot \frac{\mathrm{d}^{s_1}P_{\varphi_1}(\zeta)}{\mathrm{d}\zeta^{s_1}} \cdot \frac{\mathrm{d}^{s_2}P_{\varphi_2}(\zeta)}{\mathrm{d}\zeta^{s_2}} \cdot \frac{\mathrm{d}^{s_3}P_{\varphi_3}(\zeta)}{\mathrm{d}\zeta^{s_3}}\,\mathrm{d}\zeta \tag{A.5b}$$

$$\hat{E}^{s_1,s_2}_{\lambda,\varphi_1\varphi_2} = \int_{-1}^{1} \lambda(\zeta,T) \cdot \frac{\mathrm{d}^{s_1}P_{\varphi_1}(\zeta)}{\mathrm{d}\zeta^{s_1}} \cdot \frac{\mathrm{d}^{s_2}P_{\varphi_2}(\zeta)}{\mathrm{d}\zeta^{s_2}}\,\mathrm{d}\zeta \tag{A.5c}$$

$$\hat{E}^{s_1,s_2}_{\mu,\varphi_1\varphi_2} = \int_{-1}^{1} \mu(\zeta,T) \cdot \frac{\mathrm{d}^{s_1}P_{\varphi_1}(\zeta)}{\mathrm{d}\zeta^{s_1}} \cdot \frac{\mathrm{d}^{s_2}P_{\varphi_2}(\zeta)}{\mathrm{d}\zeta^{s_2}}\,\mathrm{d}\zeta \tag{A.5d}$$

$$T_{\zeta,\varphi_1\varphi_2} = \int_{-1}^{1} \frac{E(\zeta,T)}{1-v(\zeta,T)} \cdot \alpha(\zeta,T)\Delta T(\zeta) \cdot P_{\varphi_1}(\zeta) \cdot P_{\varphi_2}(\zeta)\,\mathrm{d}\zeta \tag{A.6}$$

$$M_{\zeta,\varphi_1\varphi_2} = \int_{-1}^{1} \rho(\zeta) \cdot P_{\varphi_1}(\zeta)P_{\varphi_2}(\zeta)\,\mathrm{d}\zeta \tag{A.7}$$

where

$$\begin{aligned} &s_1, s_2, s_3 = 0, 1 \\ &\beta_1, \beta_2, \beta_3 = u_1, u_2, u_3 \\ &\varphi_1, \varphi_2, \varphi_3 = i, \bar{i}, j, \bar{j}, k, \bar{k}, l, \bar{l}, m, \bar{m}, n, \bar{n}, p, \bar{p}, q, \bar{q}, r, \bar{r} \end{aligned} \tag{A.8}$$

References

[1] M. Yamanouchi, M. Koizumi, T. Hirai, I. Shiota, *Proceedings of First International Symposium on Functionally Gradient Materials*, Sendai, Japan, 1990.

[2] M. Koizumi, The concept of FGM, *Ceramic Transactions, Functionally Gradient Materials* 34 (1993) 3–10.

[3] G.V. Praveen, J.N. Reddy, Nonlinear transient thermoelastic analysis of functionally graded ceramic–metal plates, *International Journal of Solids and Structures* 35 (1998) 4457–4476.

[4] J.N. Reddy, Analysis of functionally graded plates, *International Journal for Numerical Methods in Engineering* 47 (2000) 663–684.

[5] J. Yang, H.S. Shen, Vibration characteristics and transient response of sheardeformable functionally graded plates in thermal environments, *Journal of Sound and Vibration* 255 (2002) 579–602.

[6] X.L. Huang, H.S. Shen, Nonlinear vibration and dynamic response of functionally graded plates in thermal environments, *International Journal of Solids and Structures* 41 (2004) 2403–2427.

[7] Y.W. Kim, Temperature dependent vibration analysis of functionally graded rectangular plates, *Journal of Sound and Vibration* 284 (2005) 531–549.

[8] J.N. Reddy, Z.Q. Cheng, Three-dimensional solutions of smart functionally graded plates, *Journal of Applied Mechanics* 68 (2001) 234–241.

[9] S.S. Vel, R.C. Batra, Three-dimensional exact solution for the vibration of functionally graded rectangular plates, *Journal of Sound and Vibration* 272 (2004) 703–730.

[10] Y.K. Cheung, D. Zhou, Three-dimensional vibration analysis of cantilevered and completely free isosceles triangular plates, *International Journal of Solids and Structures* 39 (2002) 673–687.

[11] D. Zhou, Y.K. Cheung, F.T.K. Au, S.H. Lo, Three-dimensional vibration analysis of thick rectangular plates using Chebyshev polynomials and Ritz method, *International Journal of Solids and Structures* 39 (2002) 6339–6353.

[12] Y. Miyamoto, *Functionally Graded Materials: Design, Processing and Applications*, Kluwer, Norwell, MA, 1999.
[13] R. Javaheri, M.R. Eslami, Thermal buckling of functionally graded plates, *AIAA Journal* 40 (2002) 162–169.
[14] Y.Y. Yung, D. Munz, Stress analysis in a two materials joint with a functionally graded materials. *Functionally Graded Material* (1996) 41–46.
[15] Z.H. Jin, G.H. Paulino, Transient thermal stress analysis of an edge crack in a functionally graded material, *International Journal of Fracture* 107 (2001) 73–98.
[16] Y.S. Touloukian, *Thermophysical Properties of High Temperature Solid Materials*, MacMillan, New York, 1967.
[17] G. Bao, L. Wang, Multiple cracking in functionally graded ceramic/metal coatings, *International Journal of Solids and Structures* 32 (1995) 2853–2871.
[18] L. Fox, I.B. Parker, *Chebyshev Polynomials in Numerical Analysis*, Oxford University Press, London, 1968.
[19] Q. Li, V.P. Iu, K.P. Kou, Three-dimensional vibration analysis of functionally graded material rectangular plates by Chebyshev polynomials, *Proceedings of the Tenth International Conference on Enhancement and Promotion of Computational Methods in Engineering and Science*, Sanya, China, August 2006.
[20] Q. Li, V.P. Iu, K.P. Kou, Three-dimensional vibration analysis of functionally graded material sandwich plates, *Journal of Sound and Vibration* 311 (2008) 498–515.